Jurnal Geografi Gea

Journal homepage: https://ejournal.upi.edu/index.php/gea

Coherence Analysis of Sentinel-1A Images in Various Land Covers

Satrio Muhammad Alif[1], Ongky Anggara[2], Vidiya Ristiana[3]

[1,2,3]Geomatics Engineering, Institut Teknologi Sumatera, Indonesia

Correspondence: E-mail: [1]satrio.muhammad@gt.itera.ac.id, [2]ongky.anggara@gt.itera.ac.id, [3]vidiya14ristiana@gmail.com

ABSTRACT

Coherence analysis is a valuable technique to assess the suitability and similarity of pixel pairs between two radar images taken at different times. In this study, we conducted a coherence analysis on a series of Sentinel-1A images acquired between 2017 to 2022 in Palembang, Indonesia, encompassing various land covers. The analysis was conducted on different land covers, including urban areas, agricultural lands, and natural terrains. The study aimed to identify land cover types with high coherence values in Sentinel-1A images, which could indicate stable or unchanged surfaces. The results show that land cover in Palembang, which has high coherence, is open land and built area. The average coherence value in the study area from 2017 to 2022 is ~0.2 to ~0.27, indicating relatively stable surfaces. This indicates that the Sentinel-1A image is very suitable for producing reliable and accurate information for both land cover types. This study is helpful as an initial consideration to utilize Sentinel-1A image for further earthquake and disaster analysis research.

ARTICLE INFO

Article History:
Submitted/Received 10 Aug 2023
First Revised 13 Sep 2023
Accepted 19 Oct 2023
First Available Online 30 Oct 2023
Publication Date 30 Oct 2023

Keywords:
Coherence,
Land Cover,
InSAR,
Sentinel-1A Image

1. INTRODUCTION

Sentinel-1A image is one of the satellites that utilizes SAR (Synthetic Aperture Radar) technology (Bioresita et al., 2021; Yusup et al., 2023). Sentinel-1A image uses a microwave sensor with a C band, which has a wavelength of 5.6 cm, so that it can penetrate clouds, not affected by weather conditions or not during the day or night (Cao et al., 2022). Sentinel-1A images can be used to study surface displacement in various regions, such as Tianjin, China (Zhang et al., 2019). However, the Sentinel-1A image is not good enough to study crustal deformation in areas of Indonesia that have many forests with dense vegetation, where Indonesia has forests with an area of around 50.9% of its land area, which are disproportionately distributed in Indonesia (KLHK, 2020; Razi et al., 2018). This is because the C band from the Sentinel-1A image is not good at penetrating measurements to the ground surface or objects under dense vegetation (Nasirzadehdizaji et al., 2021).

The data obtained from the Sentinel-1A image is the appearance of backscatter radar waves from objects or physical conditions on the earth's surface (Ullmann, 2019; Sumiati et al., 2023). The coherence value of radar images can be influenced by the backscatter volume received (Rulian et al., 2021). The higher backscatter is associated with a better level of coherence (Canisius et al., 2019). Coherence is the level of suitability or similarity of each pixel between two images taken at different times, with values between 0 and 1 (Lippl, 2018). Low coherence values are often found in forests, while high coherence values are found in built-up areas (Xiang et al., 2016). Each land cover has a different coherence value because it has different characteristics in reflecting radar waves (Santoro et al., 2010). This shows the relationship between coherence values and land cover.

Land cover is the physical appearance of the earth's surface (Derajat et al., 2020). Indonesia has a diverse land cover, supported by the fact that Indonesia is an archipelagic country consisting of land and sea. Analyzing the coherence of Sentinel-1A images across various land covers is an initial consideration in studying surface deformation in a specific area. This is crucial as the processing of Sentinel-1A images is time-consuming. Identifying the areas that can yield valuable surface displacement information before processing can significantly optimize the study time. The main objective of this research is to identify the land covers that produce high coherence of Sentinel-1A images.

2. METHODS

The locations in this study include the Sentinel-1A image data used in the city of Palembang and its surroundings **(Figure 1)**. This location was chosen as the research location because it is an area that has diverse land cover, including the waters of the Bangka Strait to the Bangka Belitung Islands. The classification of various land covers is also clearly visible and facilitates coherence analysis of land cover. In addition, this area has low elevation diversity (PUPR, 2017), and the shadow effect from InSAR due to high elevation differences can be assumed to be non-existent (Novellino et al., 2017).

The image data used is Sentinel-1A image data during 2017-2022, Single-Look Complex (SLC) type with Interferometric Wide (IW) recording mode, VV+VH polarization, and descending type (**Table 1**). Digital elevation Model Shuttle Radar Terrain Mission (DEM SRTM) data, which has a horizontal accuracy of 30 m and a vertical accuracy of 16 m (Farr et al., 2007), is used as image correction data to obtain coherence values. The land cover data used was obtained from Esri Land Cover in the form of a Sentinel-2A image for 2017-2022 with seven classification classes, which are the results of an Artificial Intelligence (AI) classification model. Land covers for six years with 42 images of land cover data will be used in this study.

DOI: https://doi.org/10.17509/gea.v23i2.61258
p- ISSN 1412-0313 e- ISSN 2549-7529

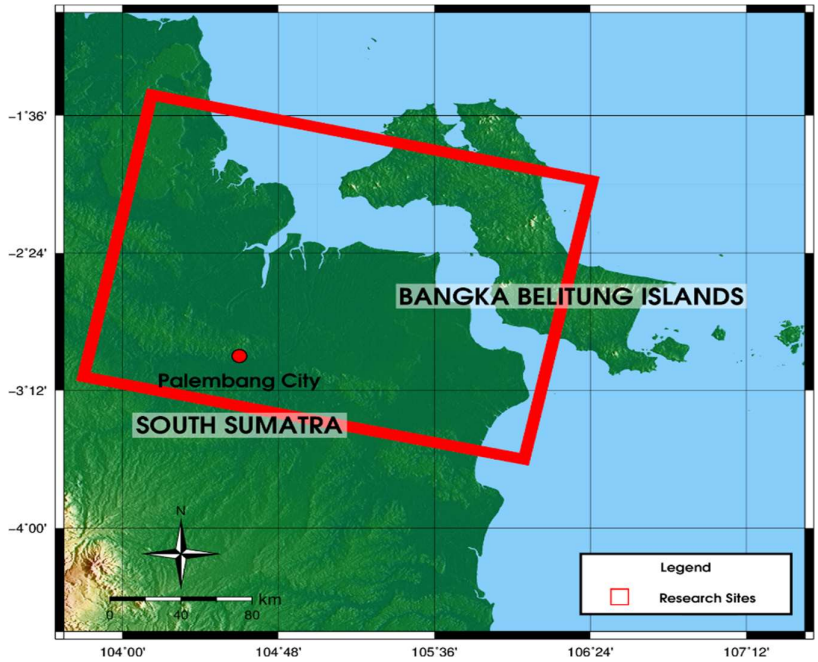

Figure 1. Map of Research Location. Red rectangle is footprint Sentinel-1A

Table 1. Sentinel-1A Image Data Specifications

Image Number	Year	Month	Date	Start of Recording	End of Recording	Image Pairs
1	2017	06	11	22:40:38	22:41:05	2, 3, 4, 5
2	2017	12	08	22:40:43	22:41:10	1, 3, 4, 5, 6
3	2018	06	06	22:40:44	22:41:11	1, 2, 4, 5, 6, 7
4	2018	12	03	22:40:50	22:41:17	1, 2, 3, 5, 6, 7, 8
5	2019	06	01	22:40:50	22:41:17	1, 2, 3, 4, 6, 8, 9
6	2019	12	10	22:40:56	22:41:23	2, 3, 4, 5, 7, 8, 9, 10
7	2020	06	07	22:40:57	22:41:24	3, 4, 5, 6, 8, 9, 10, 11,
8	2020	12	04	22:41:02	22:41:29	4, 5, 6, 7, 9, 10, 11, 12
9	2021	05	21	22:41:02	22:41:29	5, 6, 7, 8, 10, 11, 12
10	2021	12	11	22:41:08	22:41:35	6, 7, 8, 9, 11, 12
11	2022	05	04	22:41:06	22:41:33	7, 8, 9, 10, 12
12	2022	12	06	22:41:14	22:41:40	8, 9, 10, 11

DOI: https://doi.org/10.17509/gea.v23i2.61258
p- ISSN 1412-0313 e- ISSN 2549-7529

The InSAR or Interferometric Synthetic Aperture Radar method is used to process the research data. InSAR combines two SAR (Synthetic Aperture Radar) images of an area recorded at different times and recording angles to produce an interferogram image (Anggara et al., 2023). The resulting process contains phase information, and the interferogram image also contains coherence information, which will be used in this study. Then, the coherence value is obtained by validating the coherence value with land cover or the correlation **(Figure 2)**.

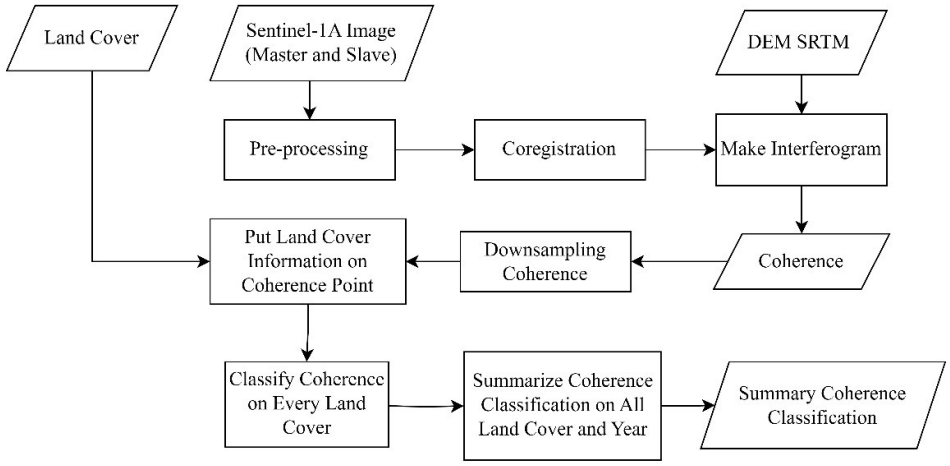

Figure 2. Flowchart of Research Implementation

The processing starts with pre-processing, such as preparing the orbits for each image, generating a baseline, and pairing the image. Then, co-registration is conducted by combining paired images into one image to form an interferogram image. In this step, each pixel (distance, azimuth) from the slave image is adjusted to the master image with 38 image pairs. The final process is to create an interferogram by forming an interferogram image and reducing topographic effects using DEM. This step produces coherence. The coherence data is downsampled every 0.2 m to reduce computation time effectively. 38 coherence data are correlated with 42 land cover data from different times. This process is conducted by assigning land cover information on each coherence pixel (Alif et al., 2020). The coherence of each land cover from 2017 to 2022 is classified from 0.18 to 0.36 with a range of 0.2. The results of the coherence classification of all images were averaged, and the average coherence value of each land cover was calculated from 2017 to 2022.

3. RESULTS AND DISCUSSION

Classification of land cover in the study area was processed according to the source of the data obtained from the Esri Land Cover website. This classification is divided into seven classes: blue as water bodies, orange as agricultural land, red as built-up land, brown as open land, yellow as shrubs/grasslands, light green as stagnant vegetation, and dark green as dense vegetation. The coherence value in this study is classified in the range of 0.18 to 0.36. The further the right of the color scale, the higher the coherence. There is a coherence value outside the classification range, but the number of pixels is very small, less than 0.09%, so it is considered an outlier. Figure 3 to Figure 8 shows the land cover and coherence map from 2017 to 2022.

DOI: https://doi.org/10.17509/gea.v23i2.61258
p- ISSN 1412-0313 e- ISSN 2549-7529

The highest coherence values are in the study areas in 2017, 2018, 2019, 2020, 2021, and 2022, which are similar values in the range 0.34-0.36, visualized in white, while the lowest coherence values are in the range 0.18-0.20, visualized in white Brown. Compared with the Land Cover Map each year, the highest coherence value is built-up land cover, while the lowest is water body land cover. Each land cover has a distribution of coherence values over a different range. Coherence in water bodies has a value between 0.18-0.24, which is visualized in brown, orange, and cream colors, especially in 2018 and 2021, with the range of coherence values in the range 0.18-0.20 more than the others. Coherence on agricultural land with stagnant vegetation, dense vegetation, and dominant grasslands/ shrubs has values in the range of 0.18-0.26, which are visualized in brown, orange, cream, and green. Coherence in dominant open land has a value between 0.18-0.30, which is visualized in brown, orange, cream, and green. Coherence on built-up land with a dominant value between 0.20-0.36.

Coherence shows the level of similarity of each pixel between image pairs in processing using the InSAR method, with a value of 0 to 1. If the coherence value is close to 1, then the coherence is getting better and will produce a good product. In the Sentinel-1A image utilizing the C band, penetration is limited when penetration through the canopy/ vegetation and water bodies, resulting in a change in the return signal (backscatter), which results in a low coherence value (Tamm et al., 2016; Olen and Bookhagen, 2018).

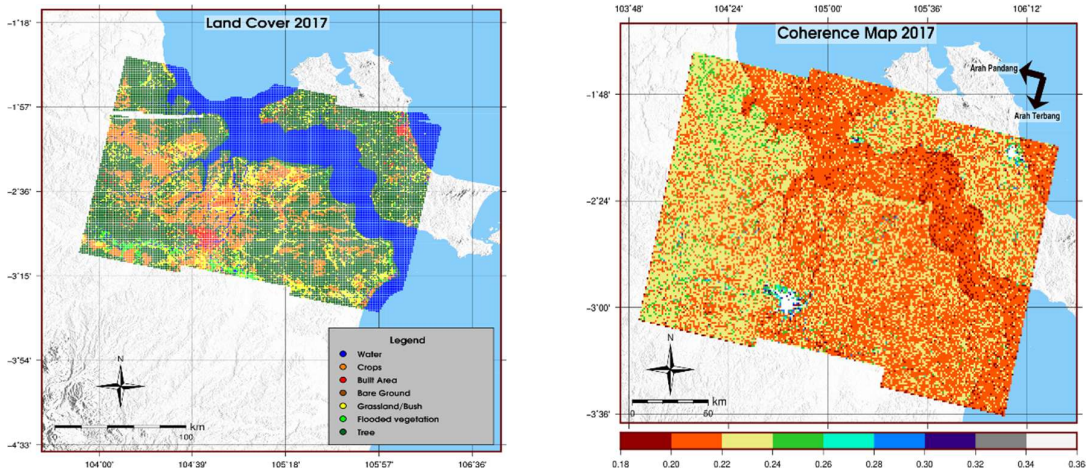

(a) (b)

Figure 3. (a) Land Cover Map 2017 and (b) Coherence Map 2017

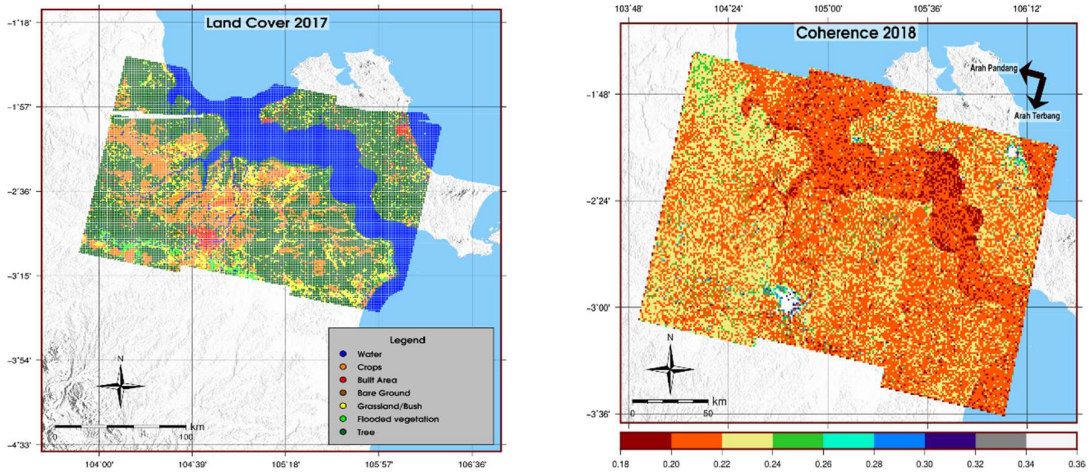

DOI: https://doi.org/10.17509/gea.v23i2.61258
p- ISSN 1412-0313 e- ISSN 2549-7529

(a) (b)

Figure 4. (a) Land Cover Map 2018 and (b) Coherence Map 2018

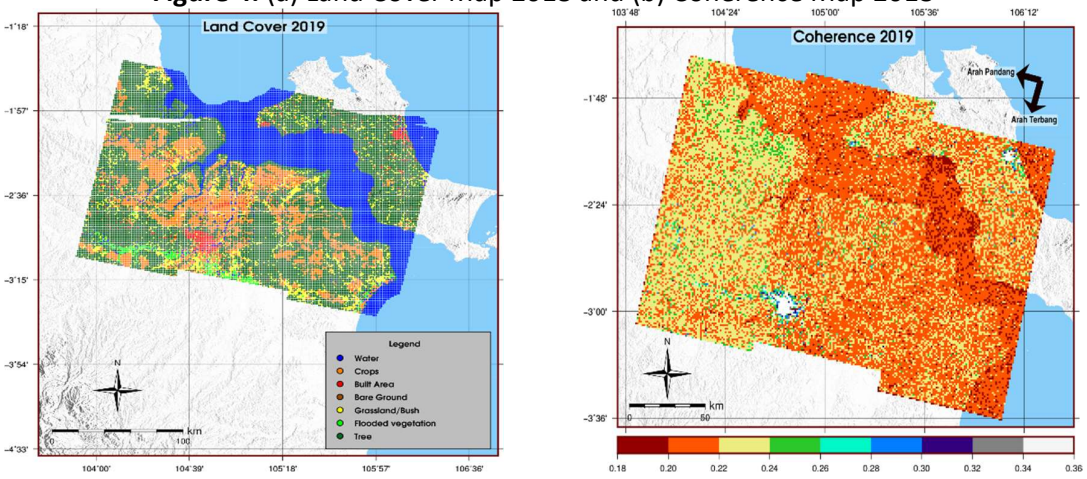

(a) (b)

Figure 5. (a) Land Cover Map 2019 and (b) Coherence Map 2019

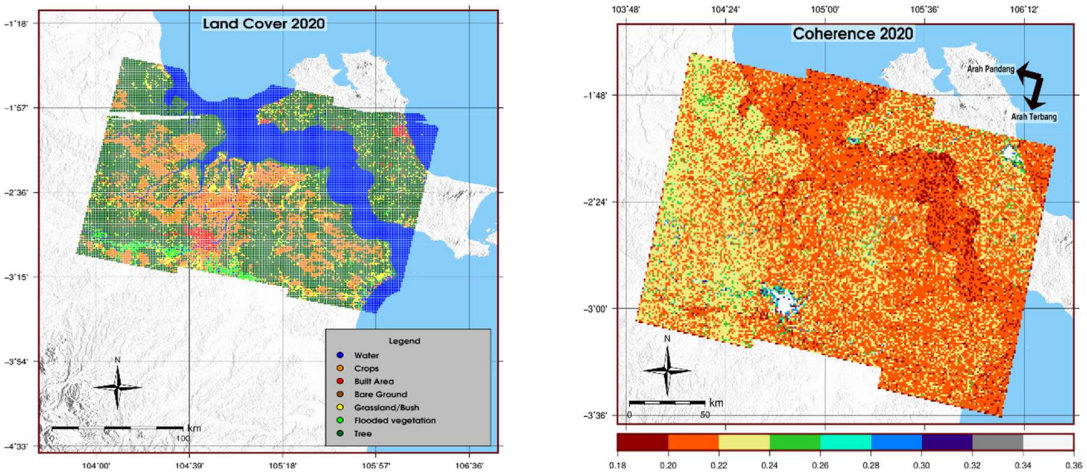

(a) (b)

Figure 6. (a) Land Cover Map 2020 and (b) Coherence Map 2020

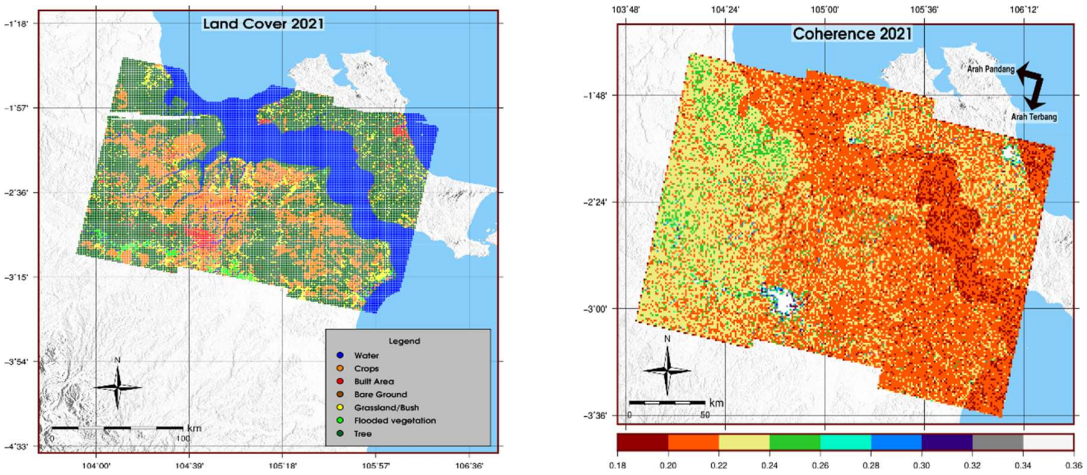

(a) (b)

Figure 7. (a) Land Cover Map 2021 and (b) Coherence Map 2022

DOI: https://doi.org/10.17509/gea.v23i2.61258
p- ISSN 1412-0313 e- ISSN 2549-7529

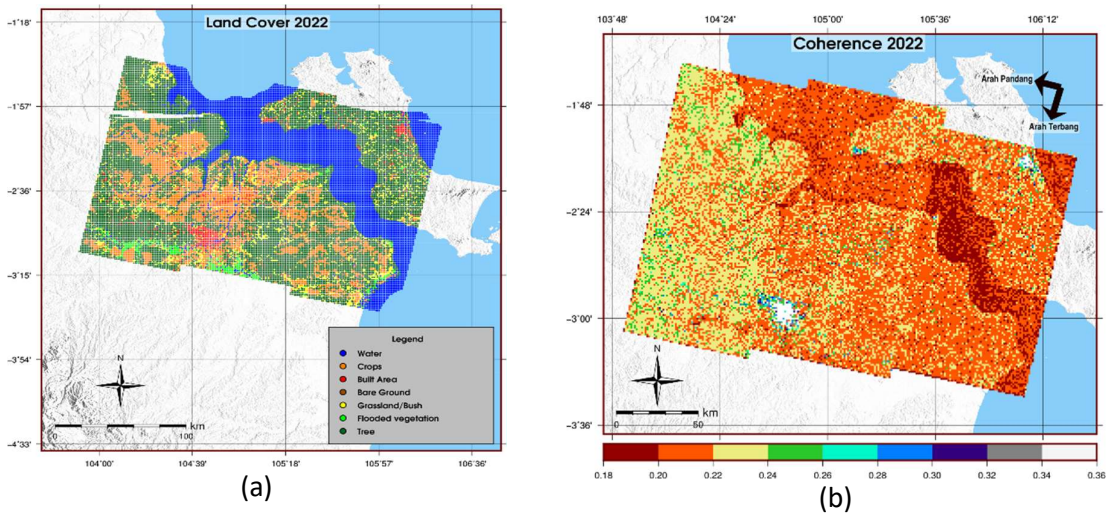

Figure 8. (a) Land Cover Map 2022 and (b) Coherence Map 2022

Table 2. The Average value of coherence in each land cover in 2017-2022

Year	Water	Crops	Built Area	Bare Ground	Flooded Vegetation	Tree	Grassland/Bush
2017	0.210	0.221	0.260	0.226	0.218	0.222	0.219
2018	0.207	0.219	0.258	0.222	0.218	0.220	0.217
2019	0.208	0.221	0.263	0.225	0.217	0.221	0.219
2020	0.208	0.220	0.263	0.224	0.216	0.220	0.218
2021	0.208	0.221	0.268	0.223	0.220	0.221	0.218
2022	0.204	0.221	0.247	0.221	0.218	0.220	0.218

Land cover in water bodies has a smaller coherence value than other land covers from 2017-2022 (**Table 2**), with an average value of 0.204 to 0.210. This is because the coherence value is affected by backscattering from the water body, and the low-value results from the characteristics of the water body. Factors that can affect the low coherence value of a body of water are that a body of water has a smooth surface, where a smooth surface will produce low backscattering because it tends to reflect microwaves in one direction, away from the direction of the sensor. In addition, in the research area, the dominant body of water is the sea area. Sea water has the ability to absorb radar waves, which can reduce backscattering. The land cover with a high coherence value is the built-up and the open land cover. The average coherence value of built-up land in 2017-2022 is 0.24 to 0.26, while the average coherence value of open land in 2017-2022 is greater than 0.22. This is because built-up land cover and open land cover are objects that produce minimum temporal decorrelation and can produce optimal backscattering and high coherence values. Therefore, the utilization of Sentinel-1A images on built-up land cover and open land cover could produce good information for further research in earthquake and disaster analysis.

DOI: https://doi.org/10.17509/gea.v23i2.61258
p- ISSN 1412-0313 e- ISSN 2549-7529

4. CONCLUSION

Sentinel-1A image coherence analysis results on various land covers from 2017 to 2022 in Palembang show that built-up and open land cover produce high coherence value. This indicates that the Sentinel-1A image is very suitable for producing reliable and accurate information for both land cover types. In contrast, the Sentinel-1A image is unsuitable for producing reliable and accurate information in areas with less open and built-up land cover and more water bodies and vegetation. The result of this study could be used as an initial consideration before utilizing Sentinel-1A image.

5. REFERENCES

Alif, S. M., Yosua, E., Fauzi, A. I., and Leksono, B. E. (2020). Association between surface air temperature and land use on the campus scale. *Journal of Geoscience, Engineering, Environment, and Technology, 5*(3), 143–150

Anggara, O., Welly, T. K., Fauzi, A. I., Alif, S. M., Perdana, R. S., Oktarina, S. W., Nuha, M. N., and Rosadi, U. (2023). Monitoring ground deformation of Sinabung volcano eruption 2018-2019 using DInSAR technique and GPS data. *AIP Publising, 2654* (1), 1–12. DOI: https://doi.org/10.1063/5.0114428

Bioresita, F., Ngurawan, M. G. R., dan Hayati, N. (2021). Identifikasi sebaran spasial genangan banjir memanfaatkan citra sentinel-1 dan google earth engine (studi kasus: banjir Kalimantan Selatan). *Journal of Geodesy and Geomatics, 17*(1), 108–118. DOI: http://dx.doi.org/10.12962/j24423998.v17i1.10383

Canisius, F., Brisco, B., Murnaghan, K., Kooij, M., and Keizer, E. (2019). SAR backscatter and insar coherence for monitoring wetland extent, flood pulse and vegetation: a study of the Amazon lowland. *Remote Sensing*, *11*(6), 1–18. DOI: https://doi.org/10.3390/rs11060720

Cao, C., Zhu, K., Song, T., Bai, J., Zhang, W., Chen, J., and Song, S. (2022). Comparative study on potential landslide identification with ALOS-2 and sentinel-1A data in heavy forest reach, upstream of the Jinsha river. *Remote Sensing, 14*(9), 1–19. DOI: https://doi.org/10.3390/rs14091962

Derajat, R. M., Sopariah, Y., Aprilianti, S., dan Taruna, A. (2020). Klasifikasi tutupan lahan menggunakan citra landsat 8 operational land imager (oli) di kecamatan Pangandaran. *Jurnal Samudra Geografi, 3*(1), 1–10. DOI: https://doi.org/10.33059/jsg.v3i1.1985

Farr, T. G., Rosen, P., Caro, E., Crippen, R., Duren, R., Hensley, S., and Burbank, D. (2007). The shuttle radar topography mission. *Advancing Earth and Space Sciences (AGU), 45*(2), 1–33. DOI: https://doi.org/10.1029/2005RG000183

Lippl, S., Vijay, S., and Braun, M. (2018). Automatic delineation of debris-covered glaciers using InSAR coherence derived from X-, C-and L-band radar data: a case study of Yazgyl Glacier. *Journal of Glaciology, 64*(247), 811–821. DOI: https://doi.org/10.1017/jog.2018.70

Nasirzadehdizaji, R., Cakir, Z., Sanli, F. B., Abdikan, S., Pepe, A., and Calo, F. (2021). Sentinel-1 interferometric coherence and backscattering analysis for crop monitoring. *Computers and Electronics in Agriculture*, *185*, 1–12. DOI: https://doi.org/10.1016/j.compag.2021.106118

Novellino, A., Cigna, F., Brahmi, M., Sowter, A., Bateson, L., and Stuart, M. (2017). Assessing the feasibility of a national InSAR ground deformation map of Great Britain with sentinel-1. *Geosciences, 7*(2), 1–14. DOI: https://doi.org/10.3390/geosciences7020019

Olen, S., and Bookhagen, B. (2018). Mapping damage-affected areas after natural hazard events using sentinel-1 coherence time series. *Remote Sensing, 10*(8), 1–19. DOI: https://doi.org/10.3390/rs10081272

Razi, P., Sumantyo, J. T. S., Perissin, D., and Kuze, H. (2018). Long-term land deformation monitoring using Quasi-Persistent Scatterer (Q-PS) technique observed by sentinel-1A: case study Kelok Sembilan. *Advances in Remote Sensing, 7*(4), 277–289.

Rulian, N., Armijon dan Murdapa, F. (2021). Analisis hamburan balik citra sentinel-1 untuk pemantauan kelas umur tanaman kelapa sawit (studi kasus: pt. perkebunan nusantara VII unit Rejosari, Natar, kabupaten Lampung Selatan). *Journal of Geodesy and Geomatics, 1*(2), 55–66.

Santoro, M., Wegmueller, U., and Askne, J.I.H. (2010). Signatures of ERS-envisat interferometric SAR coherence and phase of short vegetation: an analysis in the case of maize fields. *IEEE Transactions on Geoscience and Remote Sensing, 48*(4), 1702-1713.

Sumiati, S., Ummah, E. N. M., Fernanda, M. F., dan Ridwana, R. (2023). Perbandingan hasil metode algoritma backscattering dan otsu thresholding dalam identifikasi genangan banjir di kota Bogor. *Media Komunikasi Geografi, 24*(1), 1–14. DOI: https://doi.org/10.23887/mkg.v24i1.56080

Tamm, T., Zalite, K., Voormansik, K., and Talgre, L. (2016). Relating sentinel-1 interferometric coherence to mowing events on grasslands. *Remote Sensing, 8*(10), 1–19. DOI: https://doi.org/10.3390/rs8100802

Ullmann, T., Serfas, K., Büdel, C., Padashi, M., and Baumhauer, R. (2019). Data processing, feature extraction, and time-series analysis of sentinel-1 Synthetic Aperture Radar (SAR) imagery: examples from Damghan and Bajestan Playa (Iran). *Z Geomorphol, 62(1)*, 9–39.

Xiang, D., Tang, T., Hu, C., Fan, Q., and Su, Y. (2016). Built-up area extraction from PolSAR imagery with model-based decomposition and polarimetric coherence. *Remote Sensing, 8*(8), 1–21. DOI: https://doi.org/10.3390/rs8080685

Yusup, M., Tarigan, P. I. S., Noviansah, K., Ridwana, R., dan Aliyan, S. A. (2023). Identifikasi genangan banjir menggunakan sentinel-1 dan korelasinya dengan kerawanan banjir di kabupaten Barito Selatan. *Geo-Image, 12*(1), 62–70.

Zhang, T., Shen, W. B., Wu, W., Zhang, B., and Pan, Y. (2019). Recent surface deformation in the Tianjin area revealed by sentinel-1A data. *Remote Sensing, 11*(2), 1–25. DOI: https://doi.org/10.3390/rs11020130